Thermochimica Acta, 7 (1973) 253–260

A HIGH PRESSURE THERMOBALANCE*

J. R. WILLIAMS** AND W. W. WENDLANDT***
Department of Chemistry, University of Houston, Houston, Texas 77004 (U.S.A.)
(Received 30 May 1973)

ABSTRACT

A high pressure thermobalance was assembled by placing a DuPont Model 950 balance into a stainless steel enclosure. The thermobalance is capable of operation to a maximum pressure (of N_2) to 500 atm and to a maximum temperature of 500°C. Operation of the instrument is illustrated by the thermogravimetric curves of $BaBr_2 \cdot 2H_2O$, $CuSO_4 \cdot 5H_2O$ and $NaHCO_3$ at various pressures of nitrogen and/or carbon dioxide.

INTRODUCTION

There have been few reports in the literature of thermogravimetric investigations at pressures above one atmosphere. Information of this type is frequently useful, especially for the study of *solid–gas* type systems such as

$$\text{solid}_1 + \text{gas} \rightarrow \text{solid}_2$$

and

$$\text{solid}_1 \rightarrow \text{solid}_2 + \text{gas}$$

This technique is also useful for the study of the decomposition and vaporization of liquids where information about the rate of reaction over a wide range of temperature is required.

One of the first high pressure thermobalances was that described by Rabatin and Card[1] in 1959. It consisted of a laboratory type torsion balance enclosed in a metal chamber with a Kanthal wire wound furnace usable to a maximum temperature of 1200°C. Various gaseous atmospheres could be employed, such as N_2, O_2, H_2, CO, H_2O, CO_2 and NH_3, at pressures up to about 40 atm.

Brown et al.[2] described a high pressure instrument which consisted of a DuPont Model 950 Thermogravimetric Analyzer mounted in a pressure vessel. It could be operated to a maximum pressure of 20 atm and had a maximum usable temperature

*Taken in part from the Ph. D. Thesis of J. R. Williams, University of Houston, Houston, Texas, January, 1973.
**Present address: E. I. DuPont & Co., Victoria, Texas.
***To whom correspondence should be addressed.

of 350 °C. Other high pressure thermobalances have been described[3,4] which could be used to maximum operable pressure of 33 atm.

We wish to report here a high pressure thermobalance which is capable of operation in the pressure range from one to 500 atm in the temperature range from 25 to 500 C. A nitrogen (or carbon dioxide) atmosphere may be employed using samples with a mass of 5–20 mg.

EXPERIMENTAL

The balance assembly

The essential features of the pressure chamber enclosure balance mechanism, furnace, and accessory components are shown in Figs. 1 and 2.

The chamber was constructed of 150 mm thick bar stock of type 316 stainless steel. The 35 mm thick end plates (A) were cut from the same bar stock and eight bolt holes were drilled from the outer machined face. The inner face was also machined to obtain a close fit to the body and a 2.14 mm deep groove was cut to contain a 3.12 mm in cross-section Buna-N O-ring (B) which is used to seal the vessel. The body (C) consisted of a cylinder which was 280 mm in length with a 76 mm i.d. and 152 mm o.d. in which the ends were polished to make a good seal with the O-ring. Several threaded openings were machined into the vessel to allow entry of Conax high pressure connections for the control wires (D), sample thermocouple, furnace thermocouple (G), furnace wires (H) and gas inlet and outlet openings in the end plates (A) and (K). The end plates were bolted to the body using stainless steel hexdrive bolts, 12.7 mm diameter by 50 mm in length having five threads per cm. The balance movement (E) consisted of a taunt-band D' Arsonval-type galvanometer movement (from a DuPont thermobalance) to which a quartz arm was attached; it extended into a small furnace

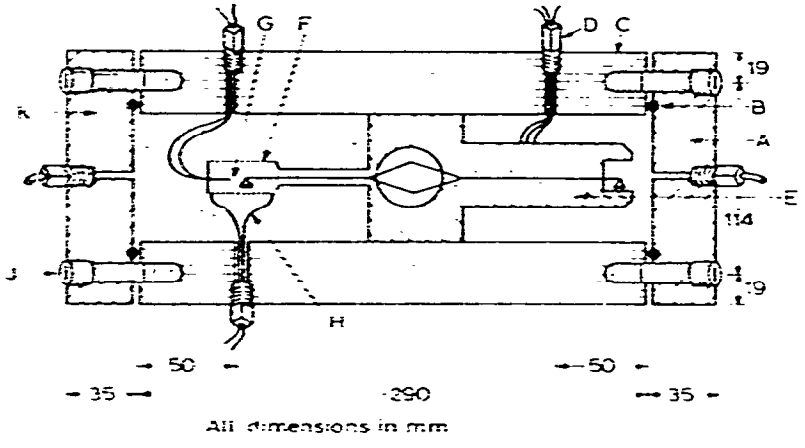

Fig. 1. Schematic diagram of the high pressure thermobalance enclosure. A, end plate with threaded opening for gas inlet fitting; B, Buna-N O-ring; C, pressure cell; D, high pressure connector for control cable; E, balance movement; F, furnace chamber; G, furnace thermocouple; H, furnace heater wire in Marinite insulation; J, hexdrive bolts; K, end plate with threaded opening for gas outlet fitting.

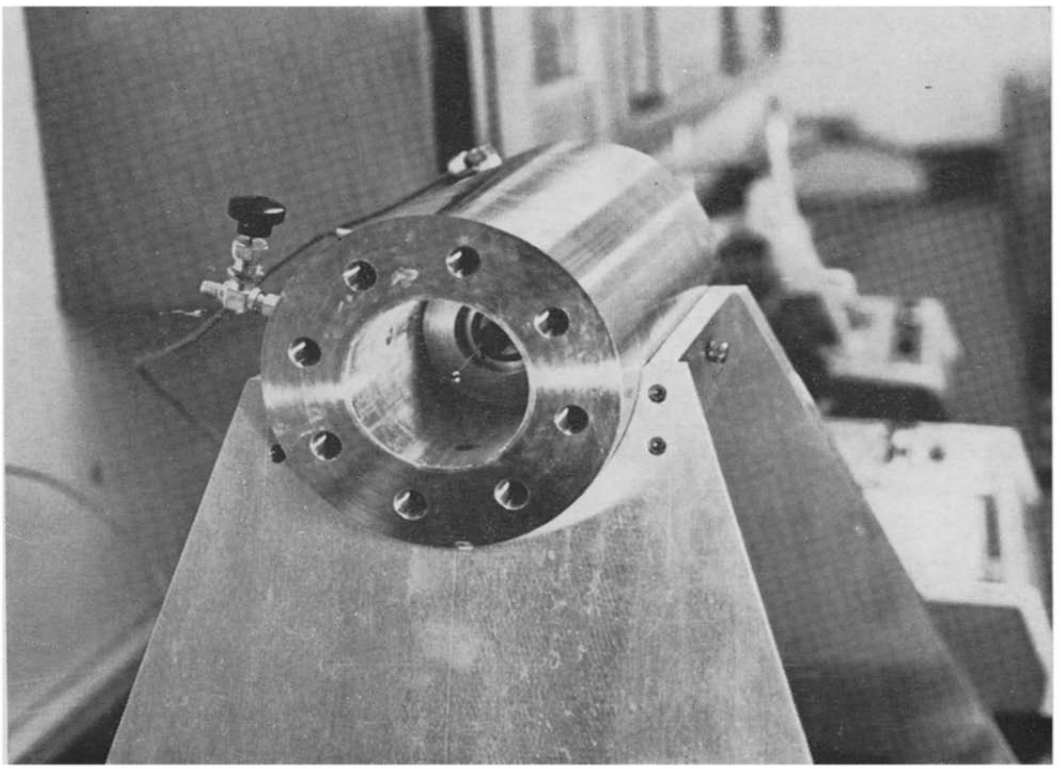

Fig. 2. High pressure enclosure for balance.

(F), and held a 0.1 ml capacity platinum sample pan. The quartz beam and pan were counterbalanced by weights at the opposite end of the beam.

The furnace was insulated with Marinite which was machined to fit the inside of the pressure vessel and extend from the inner plate to the front of the balance housing. The furnace had a minimum i.d. clearance to allow passage of the quartz balance beam and also to reduce gas turbulance. Furnace heater elements were wound from No. 26 gauge Nichrome V wire and had a total resistance of 40 ohms; No. 24 gauge Nyclad copper lead-in wires were employed. The furnace was constructed by first evenly winding the Nichrome wire on the outside of a 10 mm diameter glass tube for approximately 40 mm then covering the wire surface with a thin layer of a high temperature ceramic adhesive, "Ceramabond 503". The adhesive layer was covered with a 0.7 mm thick layer of asbestos paper and baked at 110 °C; this glass liner was then removed from the furnace by carefully drilling out the center, leaving the heater coils exposed. This method of construction resulted in a furnace with a minimum inside diameter and a maximum heat transfer capability. The furnace winding was then cemented into the insulating block and connected to the lead-in wires. It is important to note that both the sample thermocouple and the furnace thermocouple wires were routed through connections different from that of the furnace lead-in wires thus preventing a.c. voltage inductive effects.

Operation of thermobalance

A schematic diagram of the apparatus is shown in Fig. 3. Operation of the instrument consisted of the following steps: The thermobalance (A) was first balanced

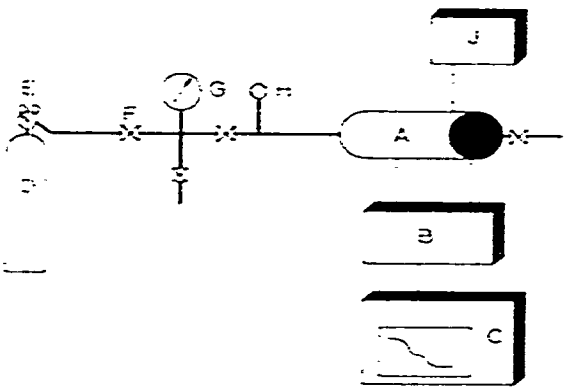

Fig. 3. Schematic diagram of thermobalance. A, thermobalance in enclosure; B, scale expansion control; C, X-Y recorder; D, gas supply cylinder; E, pressure regulator; F, control valve; G, pressure gauge; H, pressure safety release valve; J, temperature programmer.

with the sample pan in place by attaching the proper amount of weight on the opposite end of the balance. The calibration of the recorder scale was next checked and corrected by the scale expansion control (B) and the addition of the appropriate fractional analytical weights. Once calibrated, the sample was placed in the pan and the mass recorded on the recorder (C). The end insulation block was placed in the chamber and the end plate bolted in place. The chamber was then purged with the cylinder gas (D) and proper pressure of gas, as noted on the in-line gauge, was introduced (E). During operation, a slight purge of gas was maintained to insure a constant regulated pressure in the chamber.

Calibration

To calibrate the instrument, the quartz rod and sample pan were first tared by the addition of counterbalance weights that were placed on the opposite end of the beam. The thermobalance was next calibrated by placing fractional analytical weights in the sample pan. Voltage output was adjusted by the span calibration and scale expansion controls. By this means, the total response of the weight change was determined; a full scale mass response of 14 mg or 2 mg per inch was used. Since the chart could be read to about ± 0.1 division, the maximum weight sensitivity was approximately ± 0.02 mg.

RESULTS AND DISCUSSION

Effect of pressure change and heating rate

One of the serious problems encountered in using a thermobalance of this

type is the change in sample mass due to the gas buoyancy effect as the pressure is increased. It was thus very important to determine the extent to which the gas buoyancy effect contributed to the observed mass change. To do this, the volume difference between the two arms of the thermobalance was determined by measuring the position of the base line at several pressures. The initial position of the base line at 25 °C for a platinum sample pan containing aluminum oxide, as shown in Fig. 4, indicate the effect of pressure on the recorded mass change. At a pressure of 135 atm, this difference amounted to 8.4 mg at 25 °C and by applying simple gas law relations, the volume difference was calculated to be 0.053 ml.

The effect of temperature change can be seen in the curves (Fig. 5) of mass *versus* temperature for various fixed pressures. As the pressure is increased, buoyancy effects become greater; the apparent decrease in sample mass, ΔM, is given by

$$\Delta M = \varphi \Delta V \tag{1}$$

where φ is the density of the gas in the furnace chamber and ΔV is the difference in volume of the balance arms. Using the ideal gas law to relate the density to the pressure and temperature gives

$$\varphi = MP/RT \tag{2}$$

where P is the gas pressure, M the molecular weight of the gas, R the gas constant and T the absolute temperature. Combining eqns. (1) and (2) results in

$$\Delta M = \frac{MP\Delta V}{RT} \tag{3}$$

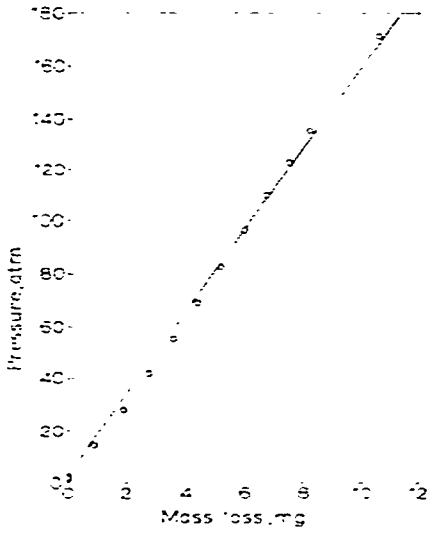

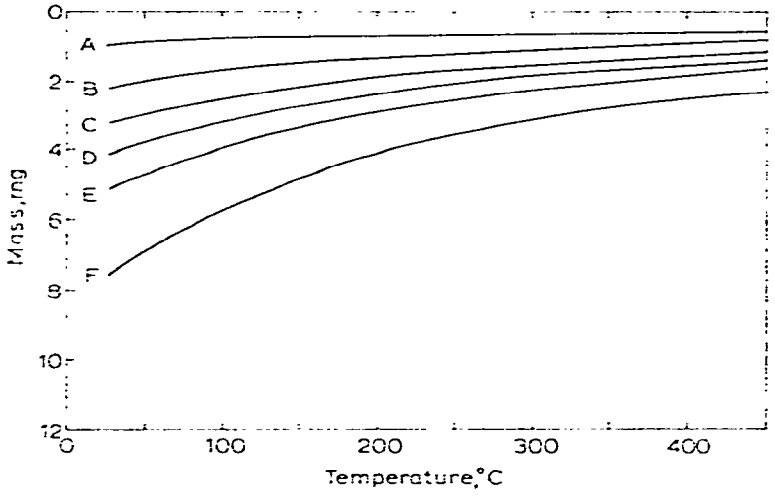

Fig. 4 (left). Apparent mass-loss as a function of systems pressure (N_2 at 25 °C).

Fig. 5 (right). Apparent mass-change as a function of temperature for fixed pressures of nitrogen; heating rate of 9 °C min^{-1}. A, 15 atm; B, 28 atm; C, 42 atm; D, 55 atm; E, 69 atm; F, 103 atm.

and obtaining the partial derivative of ΔM with respect to $1/T$ gives

$$\left[\frac{\delta M}{\delta(1/T)}\right]_P = \frac{MP\Delta V}{R} = S \tag{4}$$

Equation (4) illustrates that a plot of ΔM versus $(1/T)$ at constant pressure should be a straight line with slope S. This was observed from the experimental data for the mass change with temperature. Differentiation of S with respect to P gives

$$\left(\frac{\delta S}{\delta P}\right) = \frac{M\Delta V}{R} \tag{5}$$

Hence, a plot of ΔS versus ΔP should be a straight line with a slope of $M\Delta V/R$. From the slope of the curve, the differential volume of the balance arms, ΔV, was calculated and found to be 0.030 ml. The difference between this and the previously determined value of 0.053 is probably due to the difference in temperature of the measurements. Also, in the latter calculation, the volume difference found was an average value because of the changing gas density in the furnace area.

The buoyancy effect is easily corrected by first making a blank run to check the base line, as previously shown in Fig. 5. The effect of buoyancy as a function of temperature at constant pressure for a given sample is shown in Fig. 6 for the deaquation of $BaBr_2 \cdot 2H_2O$. In each set of curves, the original curve (A) shows a flattening effect due to the simultaneous mass-loss associated with the deaquation reaction and the mass gain due to the buoyancy effect. At the end of the run, the sample was allowed to cool at a rate equal to the initial heating rate, giving curve (B). Thus, the corrected curve (C) is obtained by substracting the buoyancy curve from the original curve.

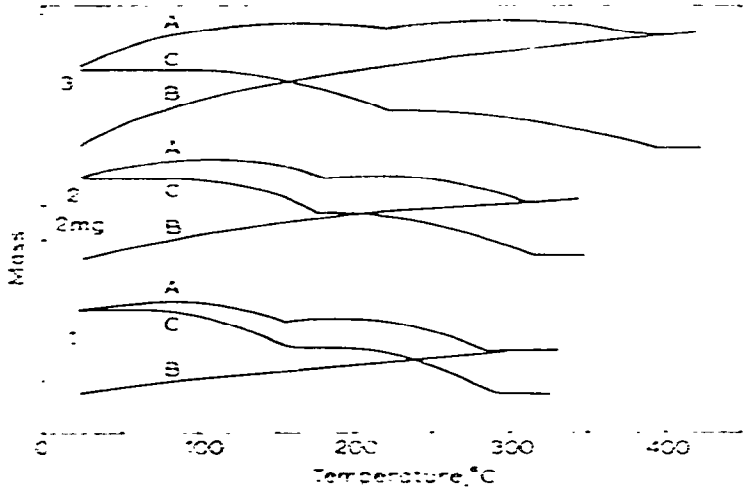

Fig. 6. Mass-loss curves for $BaBr_2 \cdot 2H_2O$ at various enclosure pressures. 1, 17 atm; 2, 35 atm; 3, 69 atm; (A) sample curve, (B) blank curve, (C) corrected curve.

Applications

The use of the thermobalance is illustrated by the TG curves of $CuSO_4 \cdot 5H_2O$ (Fig. 7) and $NaHCO_3$ (Fig. 8).

At one atm, the thermogravimetric curve for $CuSO_4 \cdot 5H_2O$ showed three distinct breaks, with the complete loss of the two moles of H_2O at 110 °C, two additional moles of H_2O at 150 °C and the final mole of H_2O at 280 °C. As can be seen, the curve breaks became less distinct and the deaquation temperature ranges increased as the pressure was increased. At 60 atm, the loss of the first two moles of H_2O was completed at 180 °C, the second two moles of H_2O at 225 °C, followed by the slow removal of the final mole of water to 425 °C. These large pressure effects are believed to be due mainly to the decreased water vapor diffusion from the sample. Although the decomposition reaction may not be greatly affected by the gas pressure, the decreased diffusion rate appears to become the rate controlling step in the deaquation reaction.

In a second example, that of the decomposition of $NaHCO_3$, similar effects were observed (Fig. 8). The final decomposition temperature increased while the temperature at which the reaction began was not greatly affected by the increase of pressure. The curve for the decomposition of the compound in 28 atm of CO_2 illustrates the effect of the presence of decomposition products (in this case CO_2) on the decomposition temperatures and reaction rates.

ACKNOWLEDGEMENT

The financial support of this work by the Robert A. Welch Foundation of Houston, Texas is gratefully acknowledged. It is also a pleasure to acknowledge the DuPont Co., Instrument Products Division, for the use of the balance mechanism.

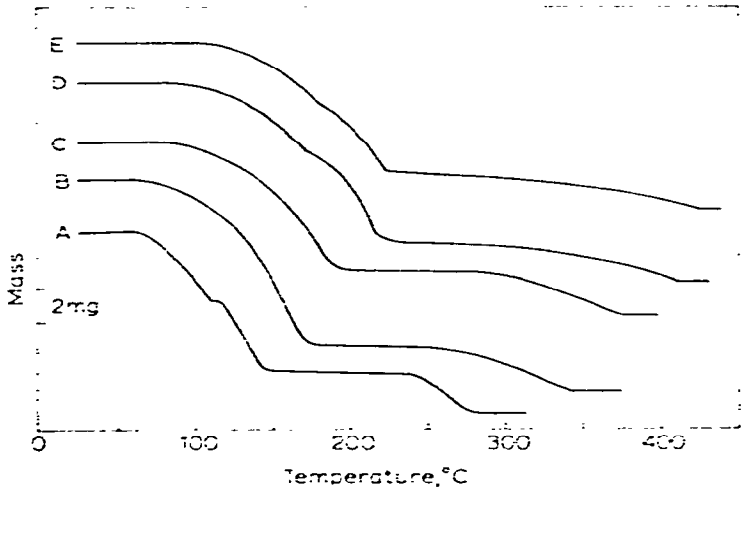

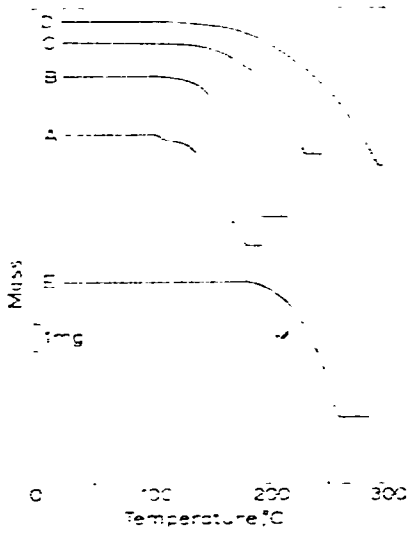

Fig. 7 (left). Effect of pressure on the dehydration of $CuSO_4 \cdot 5H_2O$: heating rate of 9 °C min^{-1}. A, 1 atm; B, 15 atm; C, 28 atm; D, 42 atm; E, 69 atm.

Fig. 8 (right). TG curves of $NaHCO_3$ at various pressures: heating rate of 9 °C min^{-1}. A, 1 atm N_2; B, 15 atm N_2; C, 42 atm N_2; D, 69 atm N_2; E, 27 atm CO_2.

REFERENCES

1 J. G. Rabatin and C. S. Card, *Anal. Chem.*, 31 (1959) 1689.
2 H. A. Brown, E. C. Penski and J. J. Callahan, *Thermochim. Acta*, 3 (1972) 271
3 W. J. Biermann and M. Heinrichs, *Can. J. Chem.*, 40 (1962) 1361.
4 H. L. Feldkirchner and J. L. Johnson, *Rev. Sci. Instrum.*, 39 (1968) 1227.